

## Design and cell cytotoxicity assessment of palmitoylated polyethylene glycol-grafted chitosan as nanomicelle carrier for paclitaxel

Sahar Abbasi,<sup>1,2</sup> Gholamhossein Yousefi,<sup>1,2</sup> Omidreza Firuzi,<sup>3</sup> Soliman Mohammadi-Samani<sup>1,2</sup>

<sup>1</sup>Department of Pharmaceutics, School of Pharmacy, Shiraz University of Medical Sciences, Shiraz, PO Box 71345-1583, Iran

<sup>2</sup>Center for Nanotechnology in Drug Delivery, School of Pharmacy, Shiraz University of Medical Sciences, Shiraz, PO Box 71345-1583, Iran

<sup>3</sup>Medicinal and Natural Products Chemistry Research Center, Shiraz University of Medical Sciences, Shiraz, PO Box 3288, 71345, Iran

Correspondence to: G. H. Yousefi (E-mail: ghyousefi@sums.ac.ir)

**ABSTRACT:** Amphiphilic graft copolymers were synthesized using chitosan with varying substitution degrees of methoxy polyethylene glycol and palmitic acid. FT-IR, <sup>1</sup>H-NMR, differential scanning calorimetry, and elemental analysis showed successful chitosan modification. Amphiphilic copolymers are able to produce nano assemblies with low critical micelle concentration (CMC). It was demonstrated that particle size (PS) analysis and drug solubilization methods could be used to determine CMC, beside fluorescent pyrene assay. Paclitaxel was efficiently loaded (up to 12.8%) without significant change in the nanomicelles' PS. In addition, without significant change in size and loading, nanomicelles could be freeze-dried. Hemolysis assay exhibited biocompatibility of copolymers and cell cytotoxicity assay on MCF-7 cell line showing the encapsulated drug had a higher cytotoxic effect. © 2015 Wiley Periodicals, Inc. *J. Appl. Polym. Sci.* **2016**, *133*, 43233.

**KEYWORDS:** biocompatibility; copolymers; drug delivery systems; micelles; polysaccharides

Received 21 July 2015; accepted 17 November 2015

DOI: 10.1002/app.43233

### INTRODUCTION

Paclitaxel (PTX) is an anticancer drug of water insoluble type with a fix position in chemotherapeutic regimens of various solid tumors, such as breast, ovarian, small and non-small cell lung cancers.<sup>1</sup> Ethanolic formulation is the first marketed formulation of PTX (Taxol<sup>®</sup>) in which Cremophor EL is used as the main surfactant.<sup>2</sup> The two most serious effects of using Cremophor EL at high concentration are neurotoxicity and hypersensitivity.<sup>3</sup> In order to overcome these problems, attempts have been made by researchers to develop systems which are able to efficiently solubilize the drug without a need for this surfactant.<sup>2</sup> In general, two main delivery systems have been developed for PTX. First, drug-polymer conjugates in which drug was conjugated to a water soluble polymer like PEG,<sup>4</sup> poly([N-(2-hydroxypropyl)methacrylamide] (HPMA),<sup>5,6</sup> polyamidoamine (PAMAM) dendrimer,<sup>7,8</sup> a polypeptide like polyglutamate,<sup>9</sup> and a peptide like bicyclic arginine-glycine-aspartic acid (RGD) peptide.<sup>10</sup> PTX-conjugated polyglutamic acid (Xyotax, CT-2103<sup>11</sup>), being developed by Cell Therapeutics, is the most promising one and is currently under third phase of clinical trials.<sup>12</sup> The second category contains PTX-loaded nanocarriers in which copolymeric nanomicelles are of a special importance.

Genexol-PM [methoxy polyethylene glycol (m-PEG)-PLA copolymeric micelle]<sup>13</sup> and NK105 (hydrophobically modified poly aspartate-PEG)<sup>14–16</sup> can be referred to as the most successful examples of this category. However, studies are still in progress in finding other polymeric materials as potential drug delivery vehicles. In this regard, chitosan and its derivatives have attracted great attention owing to their unique characteristics, e.g. biodegradability,<sup>17</sup> biocompatibility,<sup>18</sup> and accessible functional groups of hydroxyl and amine. In recent years, many investigations on chitosan modified nanomicelles have been performed, like succinylated octyl derivative,<sup>19</sup> sulfate modified octyl groups-conjugated chitosan,<sup>20,21</sup> amphiphilic cholic acid-conjugated chitosan,<sup>22</sup> chitosan-grafted vitamin E copolymer,<sup>23</sup> RGD peptide decorated PEGylated chitosan nanoparticles,<sup>24</sup> and folic acid targeted deoxycholic acid modified carboxymethylated chitosan<sup>25</sup> not only to solubilize the drug, but also to deliver it passively or actively to the desired site of tumor.

A series of hydrophilic and hydrophobic chitosan modified derivatives of medium (MCS) and low (LCS) molecular weight (MW) chitosans were designed and characterized in this research. Because of the fact that m-PEG molecules can suppress reticuloendothelial system (RES) phagocytosis by steric

hindrance and charge balance, especially in cationic nanoparticles, this approach was used for hydrophilic modification of chitosan. In order to achieve hydrogels or self-assembling nanostructures, palmitic acid (PA) had been used in several studies as a long-chain fatty acid introducing hydrophobic nature into chitosan,<sup>26</sup> trimethyl chitosan,<sup>27</sup> glycol chitosan,<sup>28</sup> and quaternary ammonium derivatives of chitosan.<sup>29,30</sup> Neither fatty acid anhydrides nor acyl chlorides were reported to be suitable because of interaction with water which makes the degree of substitution uncontrollable and leading to by-products formation. Hence, activated form of PA, palmitic-succinate (PA-NHS), were utilized<sup>31</sup> in the present study. The polymeric nanomicelles' potential in encapsulation of PTX and enhancing its water solubility was investigated. Finally, the biocompatibility and cell cytotoxicity of the most promising copolymer were evaluated through hemolysis test and thiazolyl blue tetrazolium bromide (MTT) assay. The obtained nanocarriers have the ability to improve water solubility and efficacy of PTX and other water-insoluble anticancer drugs.

## EXPERIMENTAL

### Materials

MCS from crab shells with minimum of 85% deacetylation degree, PA, m-PEG hydroxyl derivative (m-PEG-OH) (5KD), sodium cyanoborohydride (NaCNBH<sub>3</sub>), N,N-dicyclohexylcarbodiimide (DCC), N-hydroxysuccinimide (NHS), MCF-7 cell line, and MTT were purchased from Sigma-Aldrich (USA). m-PEG propionaldehyde (m-PEG-CHO) (5KD) was purchased from Jenkem (USA). PTX powder was supplied by Jinan Henry (China). RPMI 1640, Dulbecco's phosphate buffered saline (PBS), and penicillin-G/streptomycin (pen-strep) were obtained from Biosera (UK) and fetal bovine serum (FBS) was bought from Invitrogen (USA). All other solvents and material were of analytical or reagent grade and were purchased from Merck (Germany). Materials were used without further purification.

### Preparation and MW Determination of LCS

Acid hydrolysis is a convenient way to depolymerize high-MW chitosan.<sup>32</sup> According to the study of Jia and Shen, LCS was prepared via treating MCS with 85% phosphoric acid at 70°C.<sup>33</sup> To determine MW of LCS and MCS in the range of 0.03–3 mg/mL concentration, static viscosity measurements were performed using a Fenske-type viscometer (Kimax<sup>®</sup>, USA, size 200, in 25 ± 0.1°C). Sample preparation was done in 0.2M acetic acid solution in pH 5.<sup>34</sup>

### Preparation of m-PEG-CHO

m-PEG-CHO was prepared by oxidation of its hydroxyl derivative in the mixture of dimethyl sulfoxide (DMSO)/acetic anhydride according to Harris *et al.*,<sup>35</sup> and conversion degree was determined based on Schale's procedure.<sup>36</sup> Formaldehyde was used as standard reagent in this procedure. Briefly, sodium carbonate solution (0.5M, 0.6 mL) containing potassium ferricyanide (0.5 g/L) was added to increasing concentrations of formaldehyde aqueous solution (0.5 mL, 25–400 μmol/mL). The mixtures were then heated for 15 min at 100°C, and after cooling to room temperature, the optical density was determined using UV-visible spectroscopy at λ=420 nm. The optical density of the synthesized m-PEG-CHO and standard

m-PEG-CHO in 0.2 g/mL concentrations were determined under the same condition.

### Preparation of PEGylated Chitosan

To produce C-N bonds, MCS and LCS reacted to m-PEG-CHO in different mole ratios of chitosan/m-PEG followed by reduction, using NaCNBH<sub>3</sub>. In the case of MCS-PEG 1:50 (mole ratio), briefly, MCS (0.002 mmol) was dissolved in a solution of aqueous acetic acid (2% v/v) and methanol (2:1 v/v, 10 mL). The aqueous solution of m-PEG-CHO (0.1 mmol, 1 mL) was then added and mixed for 2 h at 25°C. Afterwards, the aqueous solution of NaCNBH<sub>3</sub> (0.5 mmol, 3 mL) was added drop by drop to the mixture and the solution was magnetically stirred for 24 h at 25°C. Then, the dialysis was performed with dialysis membrane (cut-off 12 KD, Sigma) for 2 days in deionized water. At the end, the purified MCS-PEG copolymers were obtained after washing the product with acetone : water (1:3 v/v). To synthesize other PEGylated derivatives, the same procedure was performed.<sup>37,38</sup>

### Preparation of PA Modified PEGylated Chitosan

In order to prepare amphiphilic chitosans, NHS ester of PA was used as an activated hydrophobic moiety. In this regard, PA solution in ethyl acetate (3.9 mmol, 20 mL) was treated with NHS (3.9 mmol) and DCC (3.9 mmol). After stirring for 20 h at 25°C, dicyclohexylurea was filtered as byproduct. The white crystals of PA-NHS were obtained through N<sub>2</sub> evaporation of solvent and recrystallization from ethanol with 90% yield.<sup>39,40</sup>

To prepare MCS-PEG-PA and LCS-PEG-PA, a certain amounts of PEGylated chitosans were added to acetic acid (0.5% v/v, 10 mL, pH 5) and were stirred for 16 h to ensure total solubility. Ethanolic solution of PA-NHS was added dropwise to the solutions at 70°C and reaction was continued for further 24 h. Subsequently, the final solutions were dialyzed first against 10% ethanol for 2 h at 40°C and 24 h at 25°C and then against deionized water at 25°C for 24 h. At last, final washing with ethanol (96%) was carried out after freeze-drying of copolymers to remove unreacted PA-NHS.<sup>41</sup>

### Characterization of Copolymers

<sup>1</sup>H-NMR analyses of intermediate compounds (m-PEG-CHO and PA-NHS) and copolymers (MCS-PEG and MCS-PEG-PA) were performed in D<sub>2</sub>O containing 1–3 drops of 20% v/v trifluoroacetic acid (for chitosan and copolymers) using a 250 MHz NMR (Bruker<sup>®</sup>, Germany). FT-IR spectroscopy was performed using VERTEX70 (Bruker<sup>®</sup>, Germany) in KBr discs. Differential scanning calorimetry (DSC) analyses were performed with empty aluminum pans as reference, using DSC302, Bahr-Thermoanalyze GmbH, Germany. The substitution degree (SD) of m-PEG and PA were determined by elemental analysis using ECS4010 elemental combustion system, Costech<sup>®</sup>, USA.

### Characterization of Nanomicelles

**Measurement of Particle Size and Zeta Potential.** Nanomicelles' particle size (PS) were determined using PS analyzer, laser diffraction model SALD-2101 (Shimadzu<sup>®</sup>, Japan). Samples of 1 mg were dissolved in 0.5% v/v acetic acid, pH 5, with the aid of bath sonication for 1 h. The zeta potentials were

measured using Zetasizer (MALVERN®, UK) in the same medium.

**Critical Micelle Concentration Determination.** The critical micelle concentration (CMC) values were determined by three different methods. In the first method, a set of nanomicelles solutions with decreasing concentrations were prepared by acetic acid (0.5% v/v) and their ability to produce response as a sign of micelle formation were evaluated by PS analyzer instrument. The second method was solubilization which determines nanomicelles loading capacity in increasing concentrations (0.01–1 mg/mL) for PTX. The third method was fluorescence assay using pyrene as a probe.<sup>20,42</sup> For this purpose, increasing concentrations of copolymers ( $0.9 \times 10^{-3}$  to 0.5 mg/mL) were prepared. After adding suitable amounts of pyrene solution (in acetone) to brown glass vials, the solvent evaporated at 30°C and suitable amount of each polymeric solution was added in order to have  $1 \times 10^{-5} M$  pyrene in each vial. The samples were allowed to rest overnight to equilibrate pyrene between two phases after 30 min of bath sonication and 2 h heating at 50°C. The emission spectra of pyrene were monitored at 360–420 nm wavelength range after excitation at 317 nm. The concentration of copolymer at breaking point of intensity ratio [369–379 nm (I/III ratio index)] versus logarithm of nanomicelles concentrations was assumed as copolymers CMC.

#### Morphological Assessment

For morphology observation of MCS-PEG-PA nanomicelles with CS : PEG : PA ratio of 1:50:600, atomic force microscopy (AFM, JPK, Germany) was applied. The sample preparation was conducted by dropping a dilute solution of nanomicelle (1 mg/mL) on cleaved clean lamella followed by drying it at 25°C for 24 h before the study. Taping mode was applied for imaging with a unilever NSC15/AIBS cantilever with constant nominal force of 40 N/m and nominal resonance frequencies of 325 kHz. Data were analyzed by Gwyddion software version 2.31.

#### Loading Efficiency and Encapsulation Efficiency of PTX

Copolymers that showed the best CMC and PS were dissolved (1 mg/mL) in acetic acid (0.5% v/v, pH 5). A certain amount of PTX solution (in acetone) was added drop by drop to polymeric solutions. Thereafter, the acetone was removed by 1 h bath sonication and further stirring at room temperature in a dark room for 3 h.<sup>43,44</sup> Samples were then bath sonicated for another 2 h and centrifuged at 3000 rpm for 5 min. The PTX loading amount in the nanomicelles (supernatant) was detected by high-performance liquid chromatography technique (HPLC). After breaking down nanomicelles by acetonitrile (3:1 volume ratio to samples), 1 min vortex mixing, 2 min bath sonication, and 10 min centrifugation in 10,000 rpm, the encapsulation efficiencies (EE %) and loading efficiencies (LE %) were calculated according to the following equations:

$$EE (\%) = \frac{\text{PTX loaded amount in copolymeric nanomicelles}}{\text{total added amount of PTX}} \times 100 \quad (1)$$

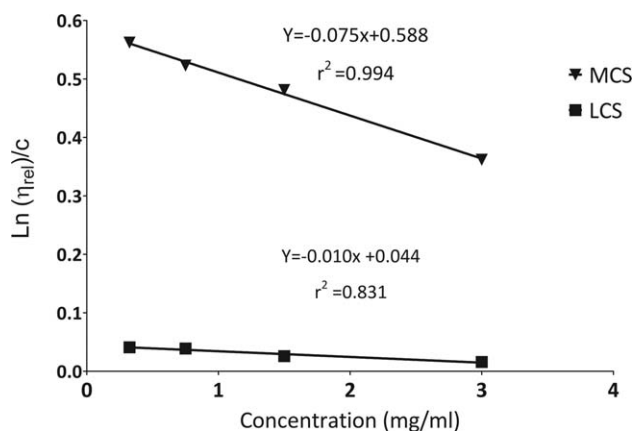


**Figure 1.** The profile of  $\ln(\eta_{rel})/c$  versus concentration in MCS and LCS dissolved in 0.1% acetic acid, used to determine MW.

$$LE (\%) = \frac{\text{PTX amount in copolymeric nanomicelles}}{\text{total added amount of copolymer}} \times 100 \quad (2)$$

#### HPLC Analysis

For drug assays, a HPLC system consisting of knauer® pump 1000, injector with loop 100 μL, UV detector S 2500 equipped with an ODS-3 Perfectsil target® MZ column (5 μm, 250 × 4.5 mm) was used. The mobile phase was acetonitrile containing deionized water (30%v/v) with 1 mL/min flow rate. Detection wavelength was set at 227 nm.

#### Biocompatibility Studies

**Hemocompatibility.** According to the study of Li *et al.*,<sup>45</sup> hemolytic activity of the optimum copolymer (1.50.600) was investigated. Considering the acetic acid incompatibility with erythrocytes, nanomicelles were prepared in normal saline using probe sonication (cycle 0.5, amplitude of 60%, Hielschre ultrasound technology).

To take blood samples, the male Sprague-Dawley rats (200–250 g) were obtained from the Laboratory Animals Research Center of Shiraz University of Medical Sciences. The animals were treated according to the guidelines of Ethics Committee of Shiraz University of Medical Sciences, ethic code no. 90-01-36-3165. Animals were anaesthetized by pentobarbital injection (50 mg/kg), and blood was collected through cardiac puncture. Blood samples were collected in 5 mL tubes containing ethylenediaminetetraacetic acid (EDTA). The plasma removal step was done by centrifugation at 700 g for 10 min followed by washing with normal saline (three times). Red blood cells pellets were then suspended in 3 mL normal saline. The copolymer concentrations of 0.1, 1, 25, 50, 100, 250, 500, and 1000 μg/mL (500 μL) were added to 50 μL of erythrocyte suspension and were maintained for 1 h at 37°C. Deionized water and normal saline solution were used as positive (C<sup>+</sup>) and negative (C<sup>-</sup>) controls, respectively. Visible spectroscopy after centrifugation at 5000 g for 15 min was used to measure hemoglobin absorbance at 540 nm. Hemoglobin release percent was calculated according to the following equation:



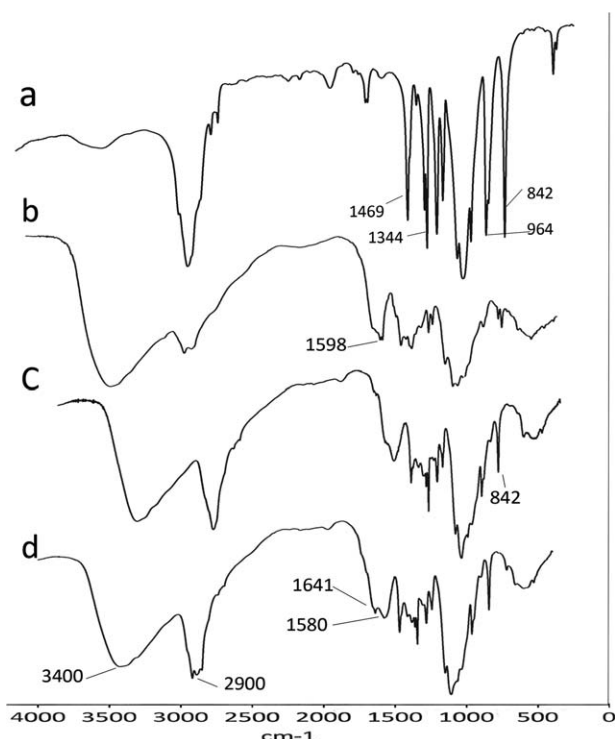


**Figure 3.** FT-IR spectra of (a) m-PEG-CHO, (b) MCS, (c) MCS-PEG, and (d) MCS-PEG-PA.

nanomicelles (copolymer concentration equal to 10, 100, and 1000 ng/mL), followed by incubation at 37°C for 72 h. Each concentration was tested in triplicate (3 wells), while nine wells were used as controls (untreated cells). Afterwards, MTT (0.5 mg/mL) was dissolved in growth medium (without phenol red) and was added to each well and after 4 h of incubation, the media was replaced with DMSO (200  $\mu$ L) in order to dissolve the formazan crystals. Finally, absorbance was measured at 570 nm (with background correction at 655 nm) and the cell viability percentage was calculated according to eq. (4). Each experiment was repeated at least three times. DMSO concentration in each well was kept below 0.1%, and proper experiments were performed to ensure that this concentration had no cytotoxic effect on the cells:

$$\text{Cell viability (\%)} = \frac{\text{Optical density of the sample}}{\text{Optical density of the control}} \times 100 \quad (4)$$

## RESULTS AND DISCUSSION

### Synthesis and Characterization of Chitosan Copolymers

Chitosan is a poor water soluble polymer, which on hydrolysis produces smaller chain polymers with higher water solubility. In the current study, phosphoric acid treatment was used as an effective technique for depolymerization of chitosan and a 10-fold reduction of its MW was obtained, as stated by Jia and Shen.<sup>33</sup> One of the best practical methods to calculate chitosan MW is based on intrinsic viscosity measurements, using Mark-Houwink-Sakurada equation<sup>47</sup> [eq. (5)], commonly used by chitosan supplier like Sigma-Aldrich. As shown in Figure 1, the  $y$ -intercepts of  $(\ln \eta_{rel}/c)$  versus concentration curves stands out for intrinsic viscosity are 0.58 and 0.044 for MCS and LCS

samples, respectively. According to Robert<sup>48</sup> and Wang<sup>34</sup> who determined  $\alpha$  as 0.93 and 0.96 and  $k$  as  $1.81 \times 10^{-3}$  and  $1.424 \times 10^{-3}$ , respectively, the viscosity-based average MW of LCS and MCS samples were calculated as 35.1 and 446.8 KD, respectively. The latter is in good agreement with the MW claimed by the supplying company, Sigma-Aldrich, 120–440 KD:

$$[\eta] = \alpha M^k \quad (5)$$

The synthetic pathway of CS-PEG-PA is briefly summarized in Figure 2. In order to produce highly stable linkages between m-PEG and chitosan NH<sub>2</sub> groups, the terminal hydroxyl group of m-PEG was transmuted to aldehyde by oxidation reaction in the mixture of acetic anhydride and DMSO. The advantage of acetic anhydride-DMSO method for m-PEG-CHO preparation is that highly hindered alcohols, which would be inert to other DMSO-activator systems (like DMSO in the presence of DCC in acidic condition), could be easily oxidized.<sup>35</sup> Schale's procedure is used to determine conversion degree which is based on ferricyanide color disappearance as a result of increasing aldehyde concentration.<sup>36</sup> The higher the amount of aldehyde groups, the lower the absorbance. A conversion degree of 84.65% was obtained based on the absorbance values of the standard and synthesized m-PEG-CHO in 20  $\mu$ mol/mL concentration. These results were close to 80% conversion degree which was reported by Harris *et al.*<sup>35</sup>

FT-IR spectra of PEGylated and palmitoylated chitosan revealed that syntheses were successfully accomplished. As shown in Figure 3, PEG has four characteristics peaks at 842, 964, 1344, and 1469  $\text{cm}^{-1}$  that all of them appeared in CS-PEG spectrum. Moreover, reduction in the intensity of peak at 1580  $\text{cm}^{-1}$  (Amide II

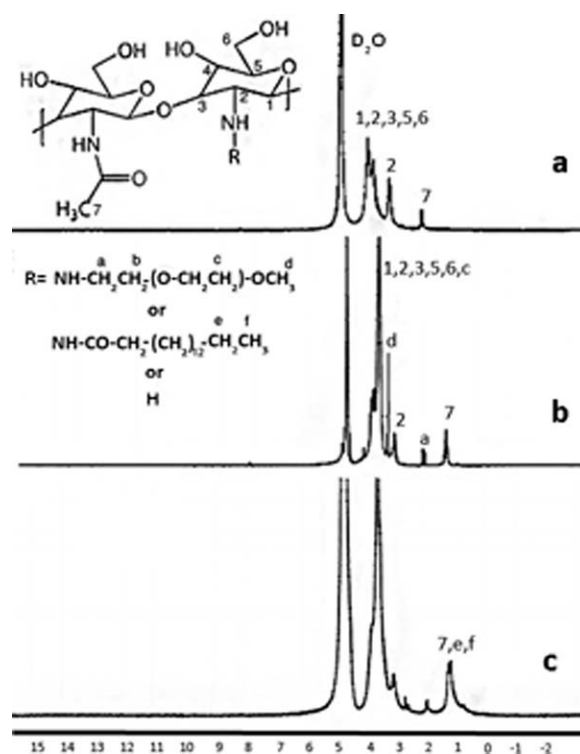


**Figure 4.** <sup>1</sup>H-NMR structural spectra of (a) MCS, (b) MCS-PEG, and (c) MCS-PEG-PA.

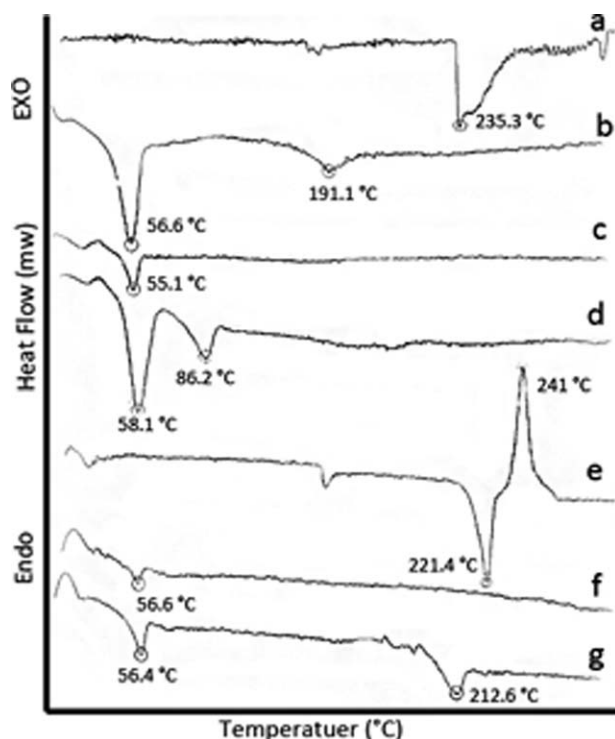


**Figure 5.** DSC thermograms of (a) MCS, (b) MCS-PEG, (c) MCS-PEG-PA, physical mixture of (d) MCS, m-PEG-CHO, and PA-NHS, (e) PTX powder, (f) PTX loaded in nanomicelles, and (g) physical mixture of PTX with copolymer powders.

of chitosan) was a further proof, indicating that PEG was successfully grafted to amine groups of chitosan. With respect to FT-IR spectra it is clear that the ratio of strong peak at  $2900\text{ cm}^{-1}$  (C-H stretch) to wide peak at  $3400\text{--}3700\text{ cm}^{-1}$  (-OH and -NH stretching vibration of MCS) increases from MCS to MCS-PEG and from MCS-PEG to MCS-PEG-PA indicating progressive modification of functional groups by alkyl chains. The successful modification of polymers in the subsequent steps of PEGylation and palmitoylation were proven by these results.

Structural modifications of chitosan were also characterized by  $^1\text{H-NMR}$  (Figure 4). The appearance of sharp singlet peak of m-PEG methyl groups at 3.4 ppm confirmed that m-PEG modification was effectively accomplished. In addition, aldehyde peak of m-PEG-CHO at 9.6 ppm was eliminated, confirming the purity of copolymers. Compared to MCS-PEG,  $^1\text{H-NMR}$  spectrum of MCS-PEG-PA showed multiple signals around 0.7 and 1.9 ppm attributed to PA methyl (-CH<sub>3</sub>) and methene (-CH<sub>2</sub>-) hydrogens, respectively, which confirms further palmitoylation.

For more investigation of the copolymers structures, DSC studies (Figure 5) were also carried out. The results showed that PEGylation does not only shifted the endothermic peak of chitosan ( $235^\circ\text{C}$ ) to lower temperature ( $191.1^\circ\text{C}$ ), but also rendered it to a less crystalline form (there is only a change in the base line after PEGylation at  $191.1^\circ\text{C}$ ). This effect was amplified by its conversion to MCS-PEG-PA ( $86.2^\circ\text{C}$  is the melting point of PA-NHS). PTX showed a sharp endothermic peak at  $221.4^\circ\text{C}$  related to fusion and a sharp exothermic peak at  $241^\circ\text{C}$  which is probably related to drug recrystallization. Nonetheless, PTX melting peak was evident in the physical mixture of PTX and nanomicelles; there was no peak in the case of PTX loaded in nanomicelles. As reported by Lian *et al.*,<sup>23</sup> and Šmejkalová *et al.*,<sup>49</sup> for PTX loaded vitamin E modified chitosan and hydrophobically modified hyaluronic acid micelles, respectively, PTX underwent a crystalline to amorphous change. This type of isomerization, as reported by Šmejkalová *et al.*, renders PTX more cytotoxic against cancerous cells.<sup>49</sup>

To determine the modification extent of chitosan by m-PEG and PA-NHS, the elemental analysis was utilized as a powerful technique to directly determine the SD by simple calculations as follows:

DS% of m-PEG groups

$$= \frac{\frac{C}{\text{Nmol in CS-PEG}} - \frac{C}{\text{Nmol in CS}}}{\text{estimated number of carbon atoms in m-PEG}} \times 100 \quad (6)$$

$$\text{DS\% of PA groups} = \frac{\frac{C}{\text{Nmol in CS-PEG-PA}} - \frac{C}{\text{Nmol in CS-PEG}}}{\text{number of carbon atoms in PA}} \times 100 \quad (7)$$

**Table I.** The SD (%) of PEG and PA in Copolymers Calculated from Elemental Analysis and the Properties of the Micelles Formed from Copolymers

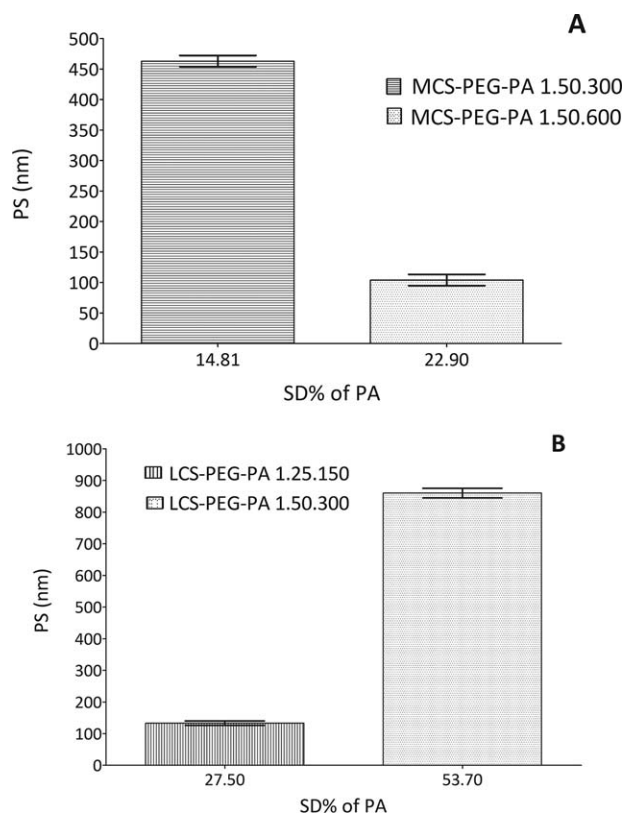
Co-polymers	CS:PEG:PA mole ratio	m-PEG SD %	PA SD %	PS±SD (nm)	PI <sup>a</sup>	CMC <sup>b</sup> (μg/mL)	CMC <sup>c</sup> (μg/mL)	CMC <sup>d</sup> (μg/mL)	Zeta potential (mV)
MCS-PEG-PA	1.50.300	0.24	14.81	463 ± 9.16	1.43	75	-	-	-
	1.100.300	0.57	25.63	115 ± 8.54	1.84	62.5	62.5	75	+25
	1.50.600	0.24	22.9	104 ± 9.16	1.96	31.25	31.2	75	+46.9
LCS-PEG-PA	1.10.30	0.36	19.5	105 ± 10.5	1.02	25.05	31.2	75	+38.4
	1.5.30	0.23	1.56	1217 ± 75.1	0.19	75	-	-	-
	1.25.150	6.08	27.5	133 ± 7.09	1.54	60.25	62.5	50-75	+39
	1.50.300	6.96	53.7	860 ± 15.3	0.21	50	-	-	-

<sup>a</sup>Polydispersity Index.

<sup>b</sup>CMC based on PS analysis method.

<sup>c</sup>CMC based on fluorescence method.

<sup>d</sup>CMC based on drug solubilization method.



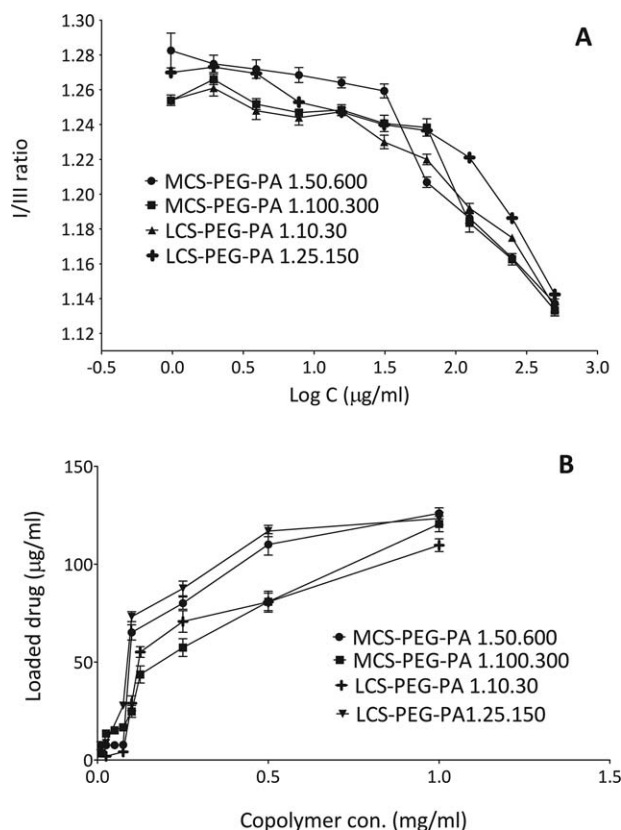
**Figure 6.** The effect of SD % of PA on PS: (A) MCS-PEG-PA and (B) LCS-PEG-PA nanomicelles.

Table I shows that in LCS copolymers, the PEGylation extent was not noticeable in low m-PEG to LCS ratios (up to 10), but increased significantly in high ratios and reached a plateau (in about 50 and 100 ratios). The results were not significantly different in MCS copolymers.

According to the results, the higher the SD % of PEG, the higher degree of palmitoylation was observed. This can be achieved in both MCS and LCS copolymers. It seems that PEGylation plays a facilitating role in further PEGylation and palmitoylation of polymer. However, in the study carried out on PEGylated N-octyl-O, N-sulfate chitosan (65 KD) by Yao *et al.*,<sup>37</sup> it was demonstrated that after an optimum degree of PEGylation (DS of 0.23), higher amounts of PEG led to lower degrees of modification with octyl groups (DS of octyl moieties were reported to be 0.41 and 0.69 in PEGylation degrees of 0.33 and 0.23, respectively). These controversial results can probably be because of the different chain length of lipophilic groups and different solubility of chitosans.

#### Nanomicelles Characteristics

PS is one of the most important factors affecting *in vitro* stability and *in vivo* fate of nanomicelles.<sup>50,51</sup> In the present study, all compounds with exception of LCS-PEG-PA 1.5.30 had sizes less than 1000 nm and some nanomicelles showed a size smaller than 150 nm. The PS of MCS-PEG-PA nanomicelles (1.50.300 and 1.50.600) in relatively same extent of PEGylation decreased with increasing SD % of PA (Figure 6). As reported by



**Figure 7.** The profiles were constructed to determine the CMC values: (A) pyrene fluorescent method and (B) drug solubilization method.

Chiu *et al.*,<sup>41</sup> who synthesized palmitoylated LCS (50 KD) with various SDs, determined by ninhydrine and poly (vinyl sulfonate) (PVSK) method, this result can be because of denser structure of the micelles formed from more hydrophobically modified polymer. However, LCS-PEG-PA nanomicelles (1.25.150 and 1.50.300) did not show the same trend (Figure 6 and Table I).

Zeta potential is an important characteristic of nanoparticles determining how a system may interact with biological

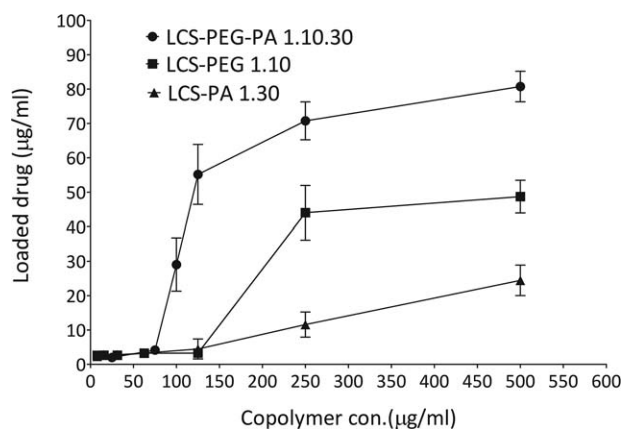


**Figure 8.** The relationships between different LCS modified copolymers concentrations and PTX loading (The solubilization method).

membranes. In current study, the zeta potential of copolymers smaller than 150 nm was measured. Considering the protonation of amine groups in acidic media, all the selected nanomicelles had positive charges. Although in the case of MCS copolymers, the difference in zeta potential was remarkable (+25 vs. +46.9 mv in 1.100.300 and 1.50.600 copolymers, respectively), and the charge differences could not be observed in the case of LCS nanomicelles in spite of the different degrees of modification (+38.4 vs. +39 mv in 1.10.30 and 1.25.150, respectively). These results were probably ascribed to the diverse MW of chitosans and the shielding effect of m-PEG molecules. Since shorter chains of LCS are shielded more intensively by m-PEG chains and shear plane moves outward, the changes in zeta potential are insignificant. In addition, MCS-PEG 1:50 had higher value of zeta potential than MCS-PEG-PA 1:50:600 (+49.7 vs. +46.9, respectively) indicating that further conjugation of amine groups, reduce the possibility of protonation and consequently, positive zeta potential diminishes in this situation.

One of the most important parameters determining the thermodynamic stability of micelles is CMC.<sup>52</sup> The CMC of copolymeric nanomicelles were determined by three methods including PS analysis, fluorescent, and solubilization. A sudden fall in I/III ratio index of pyrene in copolymers concentration range of 31.25–62.5  $\mu\text{g/mL}$  is attributed to the formation of nanomicelles in fluorescent method [Figure 7(A)]. The CMC values obtained from PS analysis method, by evaluating the lowest concentration in which the laser light PS analyzer could exhibit PS, were in good agreement with pyrene assay (Table I). The solubilization method is based on the ability of amphiphilic copolymers to solubilize the insoluble hydrophobic drugs when being assembled to form nanomicelles. As demonstrated in Figure 7(B), in a certain concentration of copolymers, a sudden raise in the amount of solubilized drug was observed as an evidence of nanomicelles formation (The CMC point). The difference between outcomes of the latter method and others may arise from the errors in measuring PTX loaded amounts and also structural differences between PTX and pyrene as a probe. Generally, the observed CMC values obtained in this research are close to the results reported by Yao *et al.*<sup>37</sup> (30–79  $\mu\text{g/mL}$ ), indicating similar copolymer structures.

According to Table I, copolymers showed PS smaller than 150 nm not only possessed lower CMC values, but also their CMC values decreased as the PA to PEG SD % ratio increased. As mentioned by Jiang *et al.*,<sup>53</sup> in addition to SD of hydrophobic groups, adjusting the balance between hydrophobic and hydrophilic groups is a significant factor. Based on the results, the two smallest copolymers of 1.50.600 and 1.10.30 that also showed the same CMC values (31.25) had PA to PEG SD % ratios of 95.41 and 54.17, respectively. However, this ratio for 1.100.300 and 1.25.150 copolymers was 44.96 and 4.5.

Furthermore, it was revealed that to produce amphiphilic copolymers capable of forming self-assembled structures, co-modification of chitosan by m-PEG and PA is more effective than modification with m-PEG or PA alone (Figure 8, Compare the different slopes of curves).

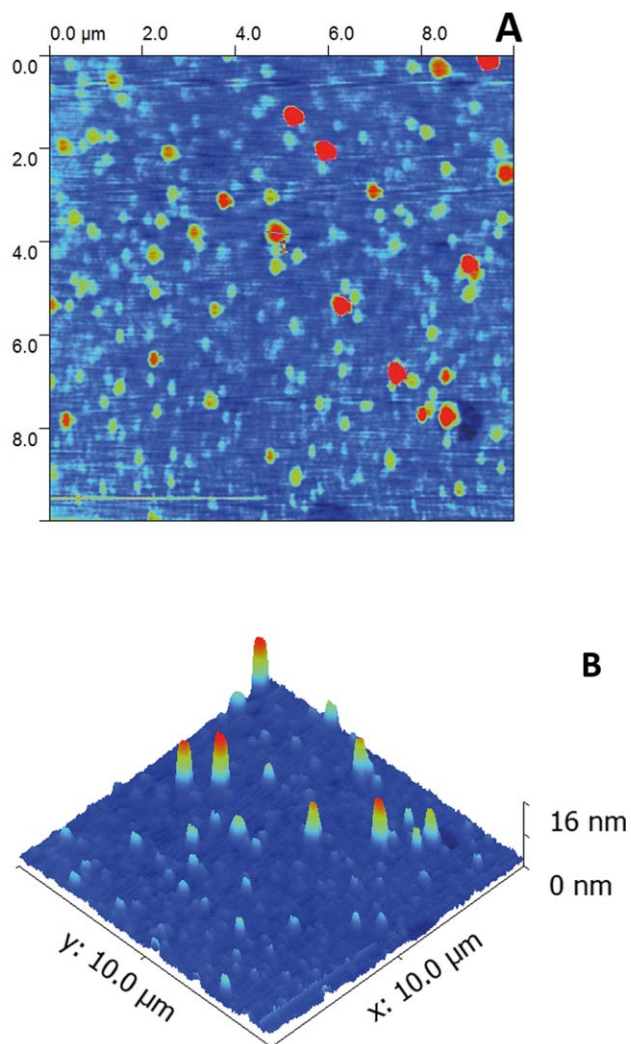


**Figure 9.** AFM images of MCS-PEG-PA 1.50.600 nanomicelles: (A) 2-D and (B) 3-D perspectives. [Color figure can be viewed in the online issue, which is available at [wileyonlinelibrary.com](http://wileyonlinelibrary.com).]

AFM has been used as a powerful technique to characterize the morphology of chitosan polymeric nanoparticles/micelles with high resolution.<sup>54</sup> The 2-D and 3-D AFM images of 1 mg/mL MCS-PEG-PA 1.50.600 nanomicelles are demonstrated in Figure 9. The average projected diameter of almost spherical (circularity value of 0.65) nanomicelles were calculated as 239 nm which increased by 2-fold when comparing hydrodynamic diameter (104 nm). This finding may be as a result of drying phase which leads to the extension of nanomicelles on the substrate surface. The calculated aspect ratio of nanomicelles was about 0.14.

The nanomicelles are kinetically unstable and tend to aggregate over time. Based on the results, MCS modified copolymers, especially 1.50.600, could produce more stable particles in contrast to LCS ones (Figure 10). This result can be attributed to longer chains of MCS-PEG-PA in comparison to LCS-PEG-PA copolymers that reduces the probability of monomer exchange among nanomicelles and make them more stable over time.<sup>55</sup>



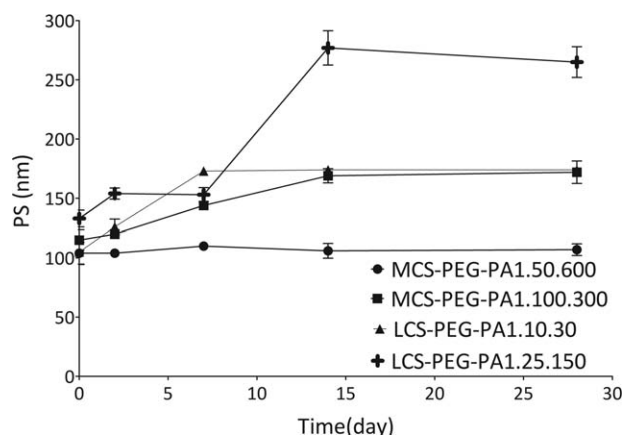


**Figure 10.** Stability of nanomicelles' PS over time.

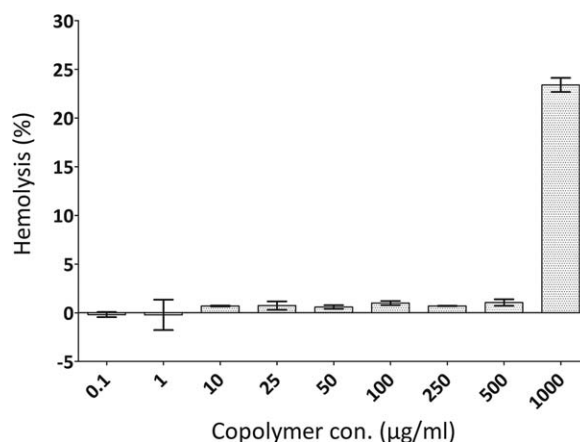


**Figure 11.** The Hemocompatibility assay of optimum copolymer, 1.50.600. Data are provided as mean  $\pm$  SD,  $n=3$ .

In addition, Gaucher *et al.*, states that “Micelle stability is also strongly related to the physical state of the core-forming polymer, be it amorphous or crystalline.”<sup>56</sup> As mentioned, limited molecular motions of the core forming groups possessing  $T_g$  higher than 37°C making micelles kinetically more stable. PA and its activated form were in crystalline state with melting points of 62°C and 86°C, respectively (Figure 5, data for PA are not provided in Figure 5). MCS-PEG-PA 1.100.300 showed higher stability than LCS-PEG-PA copolymers over time indicating slower decomposition of micelles and higher kinetic stability. The higher PA to PEG SD % ratio resulted in more stable copolymers.

#### PTX Loading Properties and Freeze-Drying Effects

Based on the results, MCS-PEG-PA 1.50.600 nanomicelles had the highest LE % and EE % of  $12.82 \pm (0.17)$  and  $91.57 \pm (1.22)$  respectively. The LE % of LCS-PEG-PA 1.25.150 nanomicelles was comparable to MCS-PEG-PA 1.50.600 ( $12.4 \pm 0.87$ ). Also, MCS-PEG-PA 1.100.300 copolymer showed LE % of about 12% and LCS-PEG-PA 1.10.30 could carry 11.2% of PTX. Drug loading amount of 12% is very promising and is comparable to capability of m-PEG modified ceramide-conjugated low molecular weight chitosan which loaded up to 11.3 of PTX<sup>57</sup> or amphiphilic cholic acid modified dihydroxypropyl chitosan micelles<sup>22</sup> with PTX maximum loading amount of 10.38%.

In another study carried out by Wang *et al.*,<sup>25</sup> folic acid targeted deoxycholic acid-conjugated carboxymethylated chitosans were reported to load about 34.67% of PTX through a self-assembled method in which both copolymer and drug were dispersed in water and nanoparticles formed by the aid of probe type sonication.

It is noteworthy that drug loading significantly increased the PS of LCS-PEG-PA nanomicelles ( $P$ -value  $\leq 0.001$ ), but was not effective on MCS-PEG-PA nanomicelles ( $P$ -value  $\geq 0.05$ ) showing more stable structure of MCS-PEG-PA copolymeric nanomicelles.

Another critical feature of a nanocarrier system for intravenous administration is its tolerance against thermal processes like freeze-drying in terms of PS and drug loading. Freeze-drying of nanoparticles is very important owing to chemical instability of drugs in liquid dosage forms.<sup>58</sup> As shown in Table II, the change in the PS of nanomicelles having LE of 7%, was significant for LCS-PEG-PA 1.25.150 and MCS-PEG-PA 1.50.600 ( $P$ -value  $\leq 0.001$  and 0.003, respectively). However, it was not significant for LCS-PEG-PA 1.10.30 and MCS-PEG-PA 1.100.300 nanomicelles ( $P$ -value = 0.86 and 1, respectively). Meanwhile, the sizes did not increase beyond 200 nm. Moreover, the results showed that the process could

**Table II.** The Effect of Freeze-Drying Process on PS and Drug Loading of 7% Drug Loaded Micelles

	PS (nm) $\pm$ SD			PTX loaded amount ( $\mu$ g/mL) $\pm$ SD	
	BL <sup>a</sup>	AL <sup>b</sup>	AF <sup>c</sup>	BF <sup>d</sup>	AF
LCS-PEG-PA 1.10.30	105 $\pm$ 10.5	261 $\pm$ 46.3	244 $\pm$ 11.7	81.84 $\pm$ 12.31	76.13 $\pm$ 1.82
LCS-PEG-PA 1.25.150	133 $\pm$ 7.09	347 $\pm$ 4.2	112 $\pm$ 8.12	65.56 $\pm$ 15.68	86.5 $\pm$ 12.35
MCS-PEG-PA 1.100.300	115 $\pm$ 8.54	127 $\pm$ 22.1	127 $\pm$ 6.4	77.29 $\pm$ 1.2	87.34 $\pm$ 12.96
MCS-PEG-PA 1.50.600	104 $\pm$ 9.16	106 $\pm$ 2.6	165 $\pm$ 6.8	78.01 $\pm$ 3.27	80.92 $\pm$ 5.78

<sup>a</sup> Before Loading.

<sup>b</sup> After Loading.

<sup>c</sup> After Freeze-drying.

<sup>d</sup> Before Freeze-drying.

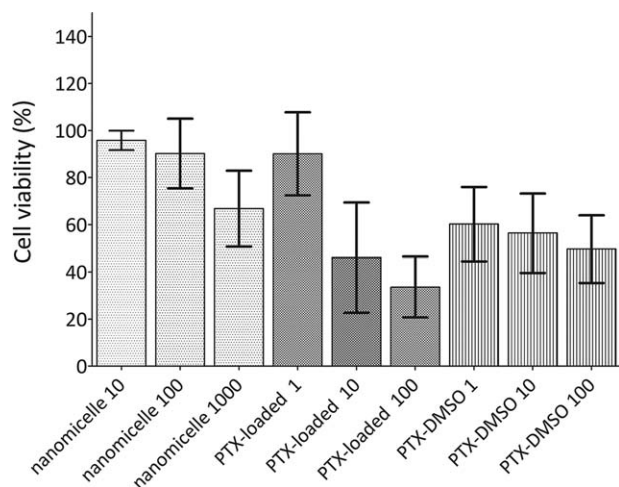


**Figure 12.** MTT-based cytotoxicity assay of DMSO-dissolved PTX (PTX-DMSO) and nanomicelles-loaded PTX (PTX-nanomicelle) at total PTX concentration of 1, 10, and 100 ng/mL and equivalent concentrations of empty nanomicelles (10, 100, and 1000 ng/mL). Data are represented as mean  $\pm$  SD for at least three replicates.

not significantly affect the LE % of nanomicelles ( $P$ -value  $>0.1$ ). Hence, freeze-drying can be used as an excellent technique for producing stable solid nanomicelle formulation from unstable drug, PTX.

#### Biocompatibility Studies

**Copolymer Hemocompatibility Assay.** The potential of CS-PEG-PA 1.50.600 as the most promising copolymer to destabilize erythrocytes as an indicator of blood compatibility was evaluated in normal saline. The hemolysis percent at copolymer concentration of 0.1–500  $\mu$ g/mL was not significantly higher than normal saline ( $P$ -value  $\geq 0.05$ ). However, 1 mg/mL concentration of copolymer showed about 23% hemoglobin release ( $P$ -value  $\leq 0.0001$ ) (Figure 11).

**Nanomicelles Cell Cytotoxicity.** The cytotoxicity studies were carried out to compare the toxicity of PTX-free and PTX-loaded nanomicelles of 1.50.600 copolymer against MCF-7 cancer cell line. Also, DMSO dissolved PTX was used for comparison. Our results showed that drug-loaded nanomicelles at 10 and 100 ng/mL concentration of PTX had a higher cytotoxic effect compared to PTX-DMSO which indicates that encapsulated drug is more effective than free drug against cancer cells (Figure 12). In addition, as shown in Figure 12, drug-free nanomicelle can be regarded as safe with more than 80% cell viability at 100 ng/mL concentration. Considering the favorable characteristics of nanomicelles such as higher blood circulation period as well as enhanced permeation and retention effect, this finding makes the present nanomicelles a promising candidate for the efficient delivery of PTX to tumors.

#### CONCLUSIONS

In this study, palmitoylated m-PEG-grafted chitosan as biocompatible and biodegradable natural polymer were prepared by simultaneous PEGylation and palmitoylation in a variety of molar ratios. A facilitating effect of PEGylation on palmitoyl-

ation of native and hydrolyzed chitosan was observed surprisingly. The results showed that in special degrees of modification, the copolymers are able to form self-assembling nanomicelles with sizes smaller than 150 nm and in the optimum one, MCS-PEG-PA 1.50.600, the size did not significantly change over long period of times. The copolymers were able to load PTX in acceptable levels and PS did not change significantly after drug loading. Additionally, the results showed that drug-loaded nanomicelles could be freeze-dried without a significant change in PS and drug loading that provides the possibility of stable formulation of PTX for long storage time. Finally, the cell studies showed acceptable hemocompatibility of empty nanomicelles and higher cytotoxicity of PTX loaded in nanomicelles than free drug, suggesting that CS-PEG-PA copolymers can be considered as a potential candidate for PTX delivery. Taking into consideration the observed limitations of marketed PTX formulations, the researchers suggest more investigations on this class of carriers as an alternative formulation strategy.

#### ACKNOWLEDGMENTS

The majority of current project was financially supported by Shiraz University of Medical Sciences, department of science and technology, research project no. 90-01-36-3165. We would like to thank Dr. Alimohammad Tamaddon for his friendly help in preparation and processing of the AFM images, Dr. Fatemeh Farjadian for her invaluable comments on reviewing the article and the research consulting center (RCC) of Shiraz University of Medical Sciences for their assistance in revising this article. The present article has been extracted from Pharm.D student thesis of Sahar Abbasi in order to fulfill the requirements of pharmacy doctorate program.

#### AUTHORS CONTRIBUTION

S. Abbasi and G.H. Yousefi designed the experiments, analyzed data, interpreted results, and wrote the paper. S. Abbasi also carried out the study. O. Firuzi guided the design, execution and analysis of the cytotoxicity assays. S. Mohammadi-Samani supervised the project. All authors have approved the submitted and read the final version of the manuscript.

#### REFERENCES

- Priyadarshini, K.; Aparajitha, U. K. *Med. Chem.* **2012**, *2*, 139.
- Singla, A. K.; Garg, A.; Aggarwal, D. *Int. J. Pharm.* **2002**, *235*, 179.
- Gelderblom, H.; Verweij, J.; Nooter, K.; Sparreboom, A. *Eur. J. Cancer* **2001**, *37*, 1590.
- Li, C.; Yu, D.; Inoue, T.; Yang, D. J.; Milas, L.; Hunter, N. R.; Kim, E. E.; Wallace, S. *Anti-Cancer Drugs* **1996**, *7*, 642.
- Etrych, T.; Sírová, M.; Starovoytova, L.; Ríhová, B.; Ulbrich, K. *Mol. Pharm.* **2010**, *7*, 1015.
- Zhang, R.; Yang, J.; Sima, M.; Zhou, Y.; Kopeček, J. *Proc. Natl. Acad. Sci.* **2014**, *111*, 12181.

7. Ma, P.; Zhang, X.; Ni, L.; Li, J.; Zhang, F.; Wang, Z.; Lian, S.; Sun, K. *Int. J. Nanomed.* **2015**, *10*, 2173.
8. He, H.; Wang, Y.; Wen, H.; Jia, X. *RSC. Adv.* **2014**, *4*, 3643.
9. Singer, J. W.; Baker, B.; de Vries, P.; Kumar, A.; Shaffer, S.; Vawter, E.; Bolton, M.; Garzone, P. *Adv. Exp. Med. Biol.* **2003**, *519*, 81.
10. Gu, G.; Gao, X.; Hu, Q.; Kang, T.; Liu, Z.; Jiang, M.; Miao, D.; Song, Q.; Yao, L.; Tu, Y. *Biomaterials* **2013**, *34*, 5138.
11. Singer, J. W.; Shaffer, S.; Baker, B.; Bernareggi, A.; Stromatt, S.; Nienstedt, D.; Besman, M. *Anti-Cancer Drugs* **2005**, *16*, 243.
12. Langer, C. J.; O'Byrne, K. J.; Socinski, M. A.; Mikhailov, S. M.; Lesniewski-Kmak, K.; Smakal, M.; Ciuleanu, T. E.; Orlov, S. V.; Dediu, M.; Heigener, D. *J. Thorac. Oncol.* **2008**, *3*, 623.
13. Ahn, H. K.; Jung, M.; Sym, S. J.; Shin, D. B.; Kang, S. M.; Kyung, S. Y.; Park, J. W.; Jeong, S. H.; Cho, E. K. *Cancer Chemother. Pharmacol.* **2014**, *74*, 277.
14. Hamaguchi, T.; Matsumura, Y.; Suzuki, M.; Shimizu, K.; Goda, R.; Nakamura, I.; Nakatomi, I.; Yokoyama, M.; Kataoka, K.; Kakizoe, T. *Br. J. Cancer* **2005**, *92*, 1240.
15. Kato, K.; Mukai, H.; Esaki, T.; Ohsumi, S.; Hozumi, Y. *J. Clin. Oncol.* **2013**, *31*, 3082.
16. Kato, K.; Chin, K.; Yoshikawa, T.; Yamaguchi, K.; Tsuji, Y.; Esaki, T.; Sakai, K.; Kimura, M.; Hamaguchi, T.; Shimada, Y. *Invest. New Drugs* **2012**, *30*, 1621.
17. Lee, K. Y.; Ha, W. S.; Park, W. H. *Biomaterials* **1995**, *16*, 1211.
18. Hirano, S.; Seino, H.; Akiyama, Y.; Nonaka, I. In *Progress in Biomedical Polymers*; Gebelein, C. G., Dunn, R. L., Eds.; Springer: New York, **1990**; Chapter 3, p 283.
19. Xiangyang, X.; Ling, L.; Jianping, Z.; Shiyue, L.; Jie, Y.; Xiaojin, Y.; Jinsheng, R. *Colloids. Surf. B Biointerfaces* **2007**, *55*, 222.
20. Zhang, C.; Qineng, P.; Zhang, H. *Colloids. Surf. B Biointerfaces* **2004**, *39*, 69.
21. Jin, X.; Mo, R.; Ding, Y.; Zheng, W.; Zhang, C. *Mol. Pharmaceut.* **2013**, *11*, 145.
22. Pan, Z.; Gao, Y.; Heng, L.; Liu, Y.; Yao, G.; Wang, Y.; Liu, Y. *Carbohydr. Polym.* **2013**, *94*, 394.
23. Lian, H.; Sun, J.; Yu, Y. P.; Liu, Y. H.; Cao, W.; Wang, Y. J.; Sun, Y. H.; Wang, S. L.; He, Z. G. *Int. J. Nanomed.* **2011**, *6*, 3323.
24. Lv, P. P.; Ma, Y. F.; Yu, R.; Yue, H.; Ni, D. Z.; Wei, W.; Ma, G. H. *Mol. Pharmaceut.* **2012**, *9*, 1736.
25. Wang, F.; Chen, Y.; Zhang, D.; Zhang, Q.; Zheng, D.; Hao, L.; Liu, Y.; Duan, C.; Jia, L.; Liu, G. *Int. J. Nanomed.* **2012**, *7*, 325.
26. Chiu, Y. L.; Chen, M. C.; Chen, C. Y.; Lee, P. W.; Mi, F. L.; Jeng, U. S.; Chen, H. L.; Sung, H. W. *Soft Matter* **2009**, *5*, 962.
27. Bei, Y. Y.; Yuan, Z. Q.; Zhang, L.; Zhou, X. F.; Chen, W. L.; Xia, P.; Liu, Y.; You, B. G.; Hu, X. J.; Zhu, Q. L. *Expert Opin. Drug Deliv.* **2014**, *11*, 843.
28. Yhee, J. Y.; Son, S.; Kim, S. H.; Park, K.; Choi, K.; Kwon, I. C. *J. Control Rel.* **2014**, *193*, 202.
29. Uchegbu, I. F.; Sadiq, L.; Arastoo, M.; Gray, A. I.; Wang, W.; Waigh, R. D.; Schätzlein, A. G. *Int. J. Pharm.* **2001**, *224*, 185.
30. Siew, A.; Le, H.; Thiovolet, M.; Gellert, P.; Schätzlein, A.; Uchegbu, I. *Mol. Pharmaceutics* **2011**, *9*, 14.
31. Chiu, Y. L.; Chen, S. C.; Su, C. J.; Hsiao, C. W.; Chen, Y. M.; Chen, H. L.; Sung, H. W. *Biomaterials* **2009**, *30*, 4877.
32. Vårum, K.; Ottøy, M.; Smidsrød, O. *Carbohydr. Polym.* **2001**, *46*, 89.
33. Jia, Z.; Shen, D. *Carbohydr. Polym.* **2002**, *49*, 393.
34. Wang, W.; Bo, S.; Li, S.; Qin, W. *Int. J. Biol. Macromol.* **1991**, *13*, 281.
35. Harris, J. M.; Struck, E. C.; Case, M. G.; Paley, M. S.; Yalpani, M.; Van Alstine, J. M.; Brooks, D. E. *J. Polym. Sci. Polym. Chem.* **1984**, *22*, 341.
36. Jarle Horn, S.; Eijssink, V. G. *Carbohydr. Polym.* **2004**, *56*, 35.
37. Yao, Z.; Zhang, C.; Ping, Q.; Yu, L. L. *Carbohydr. Polym.* **2007**, *68*, 781.
38. Sugimoto, M.; Morimoto, M.; Sashiwa, H.; Saimoto, H.; Shigemasa, Y. *Carbohydr. Polym.* **1998**, *36*, 49.
39. Lapidot, Y.; Rappoport, S.; Wolman, Y. *J. Lipid. Res.* **1967**, *8*, 142.
40. Yinsong, W.; Lingrong, L.; Jian, W.; Zhang, Q. *Carbohydr. Polym.* **2007**, *69*, 597.
41. Chiu, Y. L.; Ho, Y. C.; Chen, Y. M.; Peng, S. F.; Ke, C. J.; Chen, K. J.; Mi, F. L.; Sung, H. W. *J. Control. Release* **2010**, *146*, 152.
42. Dominguez, A.; Fernandez, A.; Gonzalez, N.; Iglesias, E.; Montenegro, L. *J. Chem. Edu.* **1997**, *74*, 1227.
43. Hu, F. Q.; Meng, P.; Dai, Y. Q.; Du, Y. Z.; You, J.; Wei, X. H.; Yuan, H. *Eu. J. Pharm. Biopharm.* **2008**, *70*, 749.
44. Hu, F. Q.; Ren, G. F.; Yuan, H.; Du, Y. Z.; Zeng, S. *Colloids. Surf. B Biointerfaces* **2006**, *50*, 97.
45. Li, X.; Yang, Z.; Yang, K.; Zhou, Y.; Chen, X.; Zhang, Y.; Wang, F.; Liu, Y.; Ren, L. *Nanoscale Res. Lett.* **2009**, *4*, 1502.
46. Shekari, F.; Sadeghpour, H.; Javidnia, K.; Saso, L.; Nazari, F.; Firuzi, O.; Miri, R. *Eur. J. Pharmacol.* **2015**, *746*, 233.
47. Kasaai, M. R.; Arul, J.; Charlet, G. *J. Polym. Sci., Part B: Polym. Phys.* **2000**, *38*, 2591.
48. Roberts, G. A.; Domszy, J. G. *Int. J. Biol. Macromol.* **1982**, *4*, 2591.
49. Šmejkalová, D.; Nešporová, K.; Hermannová, M.; Huerta-Angeles, G.; Čožíková, D.; Vištejnová, L.; Šafránková, B.; Novotný, J.; Kučerík, J.; Velebný, V. *Int. J. Pharm.* **2014**, *466*, 147.
50. He, C.; Hu, Y.; Yin, L.; Tang, C.; Yin, C. *Biomaterials* **2010**, *31*, 3657.
51. Albanese, A.; Tang, P. S.; Chan, W. C. *Annu. Rev. Biomed. Eng.* **2012**, *14*, 1.
52. Owen, S. C.; Chan, D. P.; Shoichet, M. S. *Nano Today* **2012**, *7*, 53.

53. Jiang, G. B.; Quan, D.; Liao, K.; Wang, H. *Carbohydr. Polym.* **2006**, *66*, 514.
54. Li, W.; Peng, H.; Ning, F.; Yao, L.; Luo, M.; Zhao, Q.; Zhu, X.; Xiong, H. *Food Chem.* **2014**, *152*, 307.
55. Haliloglu, T.; Bahar, I.; Erman, B.; Mattice, W. L. *Macromolecules* **1996**, *29*, 4764.
56. Gaucher, G.; Dufresne, M. H.; Sant, V. P.; Kang, N.; Maysinger, D.; Leroux, J. C. *J. Control. Release* **2005**, *109*, 169.
57. Battogtokh, G.; Ko, Y. T. *J. Drug Target* **2014**, *22*, 813.
58. Abdelwahed, W.; Degobert, G.; Stainmesse, S.; Fessi, H. *Adv. Drug Deliv. Rev.* **2006**, *58*, 1688.